

Effective merging dynamics of two and three fluid vortices: Application to two-dimensional decaying turbulence

Clément Sire, Pierre-Henri Chavanis, and Julien Sopik*

Laboratoire de Physique Théorique – IRSAMC, Université de Toulouse (UPS) and CNRS, F-31062 Toulouse, France

We present a kinetic theory of two-dimensional decaying turbulence in the context of two-body and three-body vortex merging processes. By introducing the equations of motion for two or three vortices in the effective noise due to all the other vortices, we demonstrate analytically that a two-body mechanism becomes inefficient at low vortex density $n \ll 1$. When the more efficient three-body vortex mergings are considered (involving vortices of different signs), we show that $n \sim t^{-\xi}$, with $\xi = 1$. We generalize this argument to three-dimensional geostrophic turbulence, finding $\xi = 5/4$, in excellent agreement with direct Navier-Stokes simulations [J. C. McWilliams *et al.*, *J. Fluid Mech.* **401**, 1 (1999)].

PACS numbers: 02.50.-r, 47.10.-g, 47.27.-i

Two-dimensional freely decaying turbulence (*i.e.* when an external forcing has been switched off at the initial time $t = 0$) exhibits fascinating properties [1]: starting from an initial incoherent turbulent background, robust coherent structures (the vortices) soon emerge [2–6]. Different types of structures can be observed: monopolar vortices rotating in either direction [7–9], quasi ballistic dipoles (a vortex/antivortex pair) [9, 10] and even rare tripoles (a pair of two like-sign vortices separated by an antivortex) [10]. These vortices interact due to their mutual advection which amounts to a long-range interaction. The vortices are characterized by their radius $a(t)$ and by their core (or peak) vorticity $\omega(t)$ while their precise vorticity profile is not particularly relevant in the process of 2D decaying turbulence. When two like-sign vortices approach at a critical distance of the order of their radius $a(t)$, a complex merging process occurs [11] and results in the formation of a larger vortex. As a consequence of the merging processes, the vortex density $n(t)$ decays with time while their typical size $a(t)$ increases.

Numerical simulations of the Navier-Stokes (NS) equation [6, 12–18] and of the point vortex model presented below [13, 19, 20] are consistent with experiments [21–24] in finding a power-law decay of the vortex density $n \sim t^{-\xi}$, with ξ in the range $0.6 – 1.0$, although it is most often found around $\xi \sim 0.70 – 0.75$. For an inviscid flow, the dimensional Batchelor argument [25] which assumes that the energy per unit area, $E \sim (1/L^2) \int \mathbf{u}^2 d^2 \mathbf{x} \sim \omega^2 n a^4$, is the sole invariant predicts $n \sim 1/(Et^2)$. This implies $\xi = 2$, in clear disagreement with numerical and experimental data. However, in [12], and in agreement with subsequent theoretical and experimental work, the average peak vorticity ω was also found to remain almost constant during the dynamics (see Appendix A).

The theoretical determination of the exponent ξ has been a subject of active research and many theories, based on different physical arguments – and leading in general to different results – have been proposed over the years [18, 20, 26–30]. Recently, [31] reviewed several theories and showed that some of them are inconsistent

(except that of [26] and [20]; [18] was not reviewed, since not yet published at the time) with the fact that the vortex typical velocity $v \sim \omega n^{1/2} a^2 \sim \sqrt{E}$ is constant [20].

The vortex density satisfies a general equation of the form

$$dn/dt = -n/\tau_m, \quad (1)$$

where the merging time $\tau_m(t)$ is, by definition, the typical time needed for two vortices to actually merge. Since we expect a power-law behavior for $n(t) \sim t^{-\xi}$, we conclude that $\tau_m \sim t$. Note that checking that $\tau_m \sim t$ in NS simulations or experiments is a good test to know whether the system has entered the asymptotic scaling regime [20]. In units of the collision time,

$$\tau \sim R/v \sim (\omega n a^2)^{-1}, \quad (2)$$

which is the typical time needed for a vortex of velocity $v \sim \omega n^{1/2} a^2$ [20] to travel the average inter vortex distance $R \sim n^{-1/2}$, we obtain the most general form

$$\tau_m \sim \frac{\tau}{(na^2)^\alpha} \sim \tau \left(\frac{R}{a} \right)^{2\alpha} \sim t, \quad (3)$$

where the exponent α cannot be determined on purely dimensional grounds since na^2 or R/a are dimensionless. The area fraction covered by the vortices na^2 is actually the only available dimensionless quantity [20]. Now imposing energy and peak vorticity conservation, Eq. (3) leads to

$$\xi = \frac{2}{1 + \alpha}, \quad (4)$$

so that determining ξ amounts to determining α , or the merging time τ_m . Note that Batchelor's argument [25] assumes that $\tau_m \sim \tau \sim t$, *i.e.* $\alpha = 0$, after which the energy conservation and Eq. (3) leads to $\xi = 2$, and $a \sim R \sim t$, in clear disagreement with numerical and experimental

data. Hence, the necessity of a more general scaling theory arises from the fact that the two length scales a (typical vortex radius) and R (typical inter-vortex distance) do not scale in the same way with time. In other words, the mean free time τ and the merging time τ_m are not equivalent quantities, especially at low vortex density.

We now consider the effective vortex model introduced in [12]. The exact Hamiltonian for point-like vortices can be derived from the inviscid NS equation [32] and is reminiscent of two-dimensional electrostatics

$$\mathcal{H} = - \sum_{i \neq j} \gamma_i \gamma_j \ln(|\mathbf{r}_i - \mathbf{r}_j|), \quad (5)$$

where $\gamma_i \sim \pm \omega a^2$ are the vortex circulations. The crucial difference with electrostatics resides in the fact that the vortex coordinates (x_i, y_i) are the conjugate variables, so that the resulting equations of motion are

$$\frac{dx_i}{dt} = \gamma_i^{-1} \frac{\partial H}{\partial y_i} = - \sum_{i \neq j} \gamma_j \frac{y_i - y_j}{r_{ij}^2}, \quad (6)$$

$$\frac{dy_i}{dt} = -\gamma_i^{-1} \frac{\partial H}{\partial x_i} = \sum_{i \neq j} \gamma_j \frac{x_i - x_j}{r_{ij}^2}. \quad (7)$$

Assuming that all vortices have the same conserved peak vorticity $\pm\omega$, these equations are supplemented with the following merging rules consistent with NS simulations [12, 13, 19] and experiments: when two like-sign vortices of radius a_1 and a_2 reach a distance $r_c \sim a_1 + a_2$, they merge keeping the energy $E \sim n\omega^2 a^4$ constant, so that the resulting vortex has a radius a satisfying, $a^4 = a_1^4 + a_2^4$. The average radius then scales as $a \sim (n\omega^2/E)^{-1/4} \sim t^{\xi/4} \ll R$, where $R \sim n^{-1/2} \sim t^{\xi/2}$ is the typical distance between vortices. Hence, for large time for which $a \ll R$, we expect that the application of the point-like vortex model to two-dimensional decaying turbulence becomes *more and more justified*.

The different scaling relations obtained in this work rely on the assumption that the vortices are characterized by a single length scale a . Hence, our results will be valid provided the vortex radius distribution $p(r, t)$ is integrable or marginally integrable for $r \rightarrow 0$, *i.e.* $p(r, t) \ll r^{-\delta}$, with $\delta \leq 1$. Otherwise, when the vortex size distribution is polydisperse (for $\delta > 1$), one must introduce a cut-off $r_<$ for small radii in order to ensure that $p(r, t)$ is normalizable. Then, $r_<$ and a will scale differently with time, thereby introducing another relevant length scale apart from a and R . In the case $\delta = 1$, $r_<$ and a scale identically, up to logarithmic corrections in the time t , and the present theory still applies. Starting from an incoherent initial background with an initial energy spectrum peaked at a certain scale $k_0 = 1/a_0$, experiments and NS simulations show that the radius distribution remains integrable and is very often bell-shaped (in the NS of [18], it is however claimed that $\delta = 1$) and

scale-invariant, hence satisfying

$$p(r, t) = \frac{1}{a(t)} g\left(\frac{r}{a(t)}\right), \quad (8)$$

where g is the scaling distribution and the prefactor ensures the normalization of p . Similarly, the peak vorticity distribution is found numerically and experimentally to be bell-shaped, so that only a single vorticity scale ω must be introduced.

From now on, we place ourselves in the framework of the point vortex model described above, for which we present analytical and numerical results. Hopefully, and as claimed in the two preceding paragraphs, this model is faithful enough to the original problem to apply our results to decaying turbulence in actual fluids. Our first aim is to evaluate analytically and numerically the time τ_m – hence the exponents α and ξ – necessary to observe a merging in the context of a purely *two-body* mechanism. We will then address the relevance, at least at small vortex density $na^2 \ll 1$, of *three-body* mergings (typically, a ballistic dipole hitting a single vortex), which will be shown to ultimately dominate. The numerical results of this second study will be supplemented with a fully consistent analytic mean-field three-body kinetic theory showing that the asymptotic density decay exponent should be $\xi = 1$. We finally apply a similar analytic argument to three-dimensional geostrophic decaying turbulence, finding an exponent $\xi = 5/4$ in excellent agreement with direct NS simulations [33]. The present work hence precisely assesses the crucial differences between a vortex dynamics dominated by two-body or three-body (a dipole and an isolated vortex) merging processes, demonstrating the leading role of the later at low vortex density (the importance of three-body interactions in sufficiently dilute 2D turbulence was mentioned in [34] and incorporated in kinetic models of decaying 2D turbulence in [18, 20], albeit in a different manner).

We first consider the effective dynamics of two interacting like-sign vortices, $i = 1, 2$, which are also advected by the other vortices, assumed to be uniformly distributed in space but remaining at a distance larger than R from both tagged vortices (two-body merging mechanism). Since we are ultimately interested in the regime $r = |\mathbf{r}_1 - \mathbf{r}_2| \sim a \ll R$, one can expand Eqs. (6,7) in powers of the relative distance between both vortices, r . After expressing the time in unit of τ and distances in unit of $R \sim n^{-1/2}$, we find that the relative distance between both vortices $\mathbf{r} = \mathbf{r}_1 - \mathbf{r}_2$ obeys

$$\frac{dr}{dt} = r[\cos(2\varphi)\eta_\alpha + \sin(2\varphi)\eta_\beta], \quad (9)$$

$$\frac{d\varphi}{dt} = \frac{1}{r^2} - \sin(2\varphi)\eta_\alpha + \cos(2\varphi)\eta_\beta, \quad (10)$$

where we have used cylindrical coordinates $\mathbf{r} = (x, y) = (r, \varphi)$ and the fictitious particle at \mathbf{r} is now confined to

a disk of radius $R = 1$. Furthermore, η_α and η_β represent the effective noise due to all other vortices, and are explicitly given by

$$\eta_\alpha = \sum_{j \neq 1,2} \gamma_j \frac{2x_{0j}y_{0j}}{r_{0j}^4}, \quad \eta_\beta = \sum_{j \neq 1,2} \gamma_j \frac{y_{0j}^2 - x_{0j}^2}{r_{0j}^4}, \quad (11)$$

where $\mathbf{r}_0 = (x_0, y_0)$ is the position of the center of mass of the two vortices. In the absence of the other vortices ($\eta_\alpha = \eta_\beta = 0$), the two tagged vortices would rotate around each other remaining at a constant distance r . Moreover, even in the presence of the other vortices, $dr/dt \rightarrow 0$ as $r \rightarrow 0$, since if both vortices were at the same position, they would experience the very same advection from the other vortices. The noises can be shown to satisfy [20]

$$\langle \eta_\alpha^2(t) \rangle = \langle \eta_\beta^2(t) \rangle \sim \tau^{-2}, \quad \langle \eta_\alpha(t) \eta_\beta(t') \rangle = 0, \quad (12)$$

where $\tau^{-2} \sim \mathcal{O}(1)$ in our dimensionless units. Moreover, these noises only vary notably on the time scale over which the other vortices travel a distance of order R . Their correlation time is thus of order $\tau \sim \mathcal{O}(1)$ [20]. The fact that this correlation time is non-zero (as it would be for a standard pure white noise) is crucial: when the two vortices are very close to each other, their mutual rotation period will become much smaller than τ , which will result in the effective averaging out of the external noises $\eta_{\alpha,\beta}$. Finally, it appears reasonable to modelize η_α and η_β by effective Ornstein-Uhlenbeck processes [20, 35] with variance and correlation time both equal to 1:

$$\frac{d\eta_\gamma}{dt} = -\eta_\gamma + \sqrt{2}w_\gamma, \quad \gamma = \alpha, \beta, \quad (13)$$

where w_α and w_β are two independent δ -correlated Gaussian white noises, implying $\langle \eta_\gamma(t) \eta_{\gamma'}(t') \rangle = e^{-|t-t'|} \delta_{\gamma,\gamma'}$. The Fokker-Planck equation associated to the system of Eqs. (9,10,13), which describes the evolution of the probability distribution function (*pdf*) of the variables $(r, \varphi, \eta_\alpha, \eta_\beta)$, can be easily written (see Appendix B). Unfortunately, it seems unlikely that its general time-dependent solution can be analytically obtained. However, it is straightforward to check that $P(r, \varphi, \eta_\alpha, \eta_\beta) \propto r e^{-\eta_\alpha^2/2 - \eta_\beta^2/2}$ is a stationary solution. Hence, the relative coordinate $\mathbf{r} = (x, y)$ has a uniform asymptotic distribution.

For $r \ll 1$, we can still obtain some useful information on $P(r, t)$, since the stochastic term in Eq. (10) can be neglected with respect to r^{-2} in this regime. Dividing Eq. (9) by Eq. (10), and integrating over φ , we obtain

$$\frac{1}{r^2(t)} - \frac{1}{r^2(0)} \sim \int_{\varphi_0}^{\varphi} [\cos(2\varphi')\eta_\alpha(\varphi') + \sin(2\varphi')\eta_\beta(\varphi')] d\varphi'. \quad (14)$$

Hence, for small r , the variable r^{-2} has approximately a Gaussian distribution (being the linear sum of Gaussian

variables η_α and η_β) of variance

$$\int_{\varphi_0}^{\varphi} d\varphi_1 \int_{\varphi_1}^{\varphi} d\varphi_2 \cos[2(\varphi_2 - \varphi_1)] e^{-|t(\varphi_2) - t(\varphi_1)|}. \quad (15)$$

Since $t'(\varphi) \approx r^2(\varphi) \ll 1$, we can write $t(\varphi_2) - t(\varphi_1) \sim (\varphi_2 - \varphi_1)t'(\varphi_1)$. Finally, after computing the integral in Eq. (15) in the limit of large ϕ ,

$$\begin{aligned} \int_{\varphi_1}^{\varphi} d\varphi_2 \cos[2(\varphi_2 - \varphi_1)] e^{-(\varphi_2 - \varphi_1)t'(\varphi_1)} &= \frac{t'(\varphi_1)}{4 + t'^2(\varphi_1)} \\ &\approx \frac{t'(\varphi_1)}{4}, \end{aligned} \quad (16)$$

we find, using Eq. (14), and for large φ and time t

$$\left\langle \left(\frac{1}{r^2(t)} - \frac{1}{r^2(0)} \right)^2 \right\rangle \sim \frac{1}{4} \int_{\varphi_0}^{\varphi} t'(\varphi_1) d\varphi_1 \sim \frac{t}{4}. \quad (17)$$

Remembering that the asymptotic *pdf* is $P(r) \sim r$ and that the random variable r^{-2} is approximately Gaussian for small r , the above argument suggests that $P(r, t)$ can be written as

$$P(r, t) = r f[r/r_0(t)], \quad r_0(t) \sim t^{-1/4}, \quad f(x) \sim e^{-x^{-4}}, \quad (18)$$

where the typical scale $r_0(t) \sim t^{-1/4}$ has been deduced from Eq. (17).

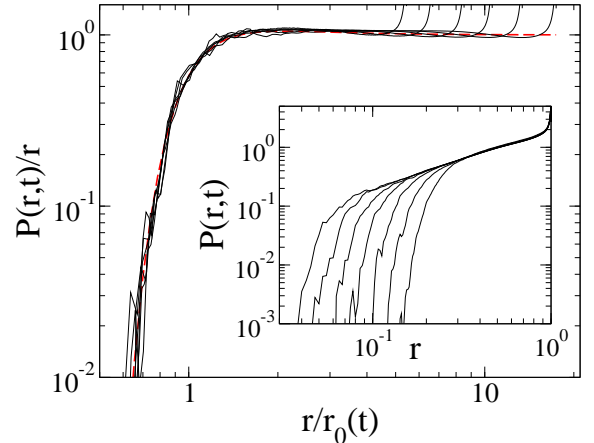


FIG. 1. (Color online) Insert: we plot $P(r, t)/r$ for 7 different times (in geometric progression) up to $t \sim 10^5$, averaged over trajectories starting from $r(0) \sim 1$. The main plot shows the corresponding data collapse, fully consistent with Eq. (18), along with a fit to the predicted Gaussian functional form (in the variable x^{-2}) for the scaling function, $f(x) = e^{-(x^{-2} - x_0^{-2})^2}$ ($x_0 \approx 2.1$; dashed line).

This scaling behavior is illustrated in Fig. 1, where Eqs. (9,10,13) have been solved numerically using a second order stochastic integration scheme. We ran $\sim 10^5$ trajectories up to $t \sim 10^5$, starting from random initial values for $r(0) \sim 1$ ($R = 1$ in our units) and $\phi(0)$ (uniformly distributed in $[0, 2\pi]$). The distribution of $r(t)$,

$P(r, t)$, is plotted for seven different times, illustrating the perfect scaling collapse predicted by Eq. (18).

Using Eq. (18), we can obtain the behavior of the moments of $r(t)$ for large time. We find that for $z > -2$, $m_z(t) = \langle r^z(t) \rangle$ converges to a constant, while $m_{-2}(t) \sim \ln t$, and

$$m_z(t) \sim t^{-(z+2)/4}, \text{ for } z < -2. \quad (19)$$

In addition, Eq. (10) implies $\langle \varphi(t) \rangle \sim t \langle r^{-2}(t) \rangle \sim t \ln t$. These different predicted behaviors are in excellent agreement with numerical simulations of Eqs. (9,10,13) presented in Fig. 2.

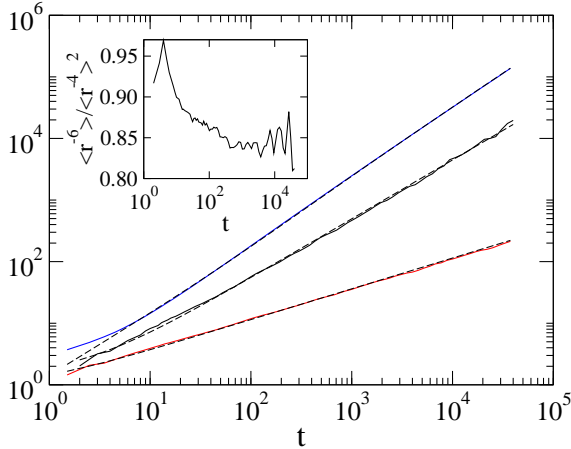


FIG. 2. (Color online) From bottom to top, we plot $m_{-4}(t) = \langle r^{-4}(t) \rangle$, $\exp(\langle r^{-2}(t) \rangle)$ (which should have a power-law behavior, since $m_{-2}(t) \sim \ln t$), and $\langle \varphi(t) \rangle$. The dashed lines are fits to the predicted functional forms (see text): $a_0 t^{a_1}$ for $\exp[m_{-2}(t)]$ and $m_{-4}(t)$ (in this case, $a_1 = 0.49(1)$), and $a_0 t \ln(t + a_1)$ for $\langle \varphi(t) \rangle$. The Insert illustrates the near constancy of $m_{-6}(t)/m_{-4}^2(t)$, which is also fully consistent with $r_0(t) \sim t^{-1/4}$ and the scaling form of $P(r, t)$ in Eq. (18).

Let us now address the problem of determining the merging time $\tau_m(r_c)$ for two vortices of radius r_c starting at a distance $r(0) \sim 1$, both lengths being expressed in unit of R . By definition, $\tau_m(r_c)$ is the average time necessary for the distance r between the two vortices to reach the value r_c for the first time. Alternatively, defining $r_{\min}(t)$ as the minimum $r(t)$ reached up to time t , one should have

$$\langle r_{\min}(\tau_m(r_c)) \rangle \sim r_c, \quad (20)$$

and one can obtain an estimate of $\tau_m(r_c)$ by inverting this relation. Moreover, our previous heuristic argument resulting in Eq. (17) actually shows that the average escape time $\tau_e(r_c)$ to go from a region for which $r(0) \in [(1 - \varepsilon)r_c, r_c]$ (with $0 < \varepsilon \ll 1$) to another for which $r(t) \in [1 - \varepsilon, 1]$ is given by

$$\tau_e(r_c) \sim r_c^{-4}. \quad (21)$$

A (Markovian) detailed balance argument then implies that the typical time to go from $r(0) \in [1 - \varepsilon, 1]$ to $r(t) \in [(1 - \varepsilon)r_c, r_c]$ – a time we assimilate to $\tau_m(r_c)$ – satisfies

$$\frac{\text{Prob}(r \in [1 - \varepsilon, 1])}{\tau_m(r_c)} \sim \frac{\text{Prob}(r \in [(1 - \varepsilon)r_c, r_c])}{\tau_e(r_c)}. \quad (22)$$

Using the stationary *pdf*, $P(r) \sim r$, and the above result for $\tau_e(r_c)$, we obtain

$$\tau_m(r_c) \sim r_c^{-6}, \quad \langle r_{\min}(t) \rangle \sim t^{-1/6}. \quad (23)$$

We have numerically estimated $\langle r_{\min}(t) \rangle$ and the first-passage times $\tau_m(r_c)$ and $\tau_e(r_c)$, by integrating Eqs. (9,10,13) using a second order stochastic integration scheme (see Fig. 3). r_c being initially fixed, the merging time $\tau_m(r_c)$ is determined by averaging over $\sim 10^6$ (large r_c) to $\sim 10^5$ (smallest r_c) realizations, the first time for which the inter-vortex distance $r(t) < r_c$ (merging criterion), starting from an initial $r(0) \sim 1$. Conversely, starting from an initial $r(0) = r_c < r_{\max}$, the escape time $\tau_e(r_c)$ is estimated as the first time for which $r(t) > r_{\max} \sim 1$ (we have set $r_{\max} = 0.8$ in unit of R). The results presented in Fig. 3 are in good agreement with our analytic estimates of Eqs. (21,23).

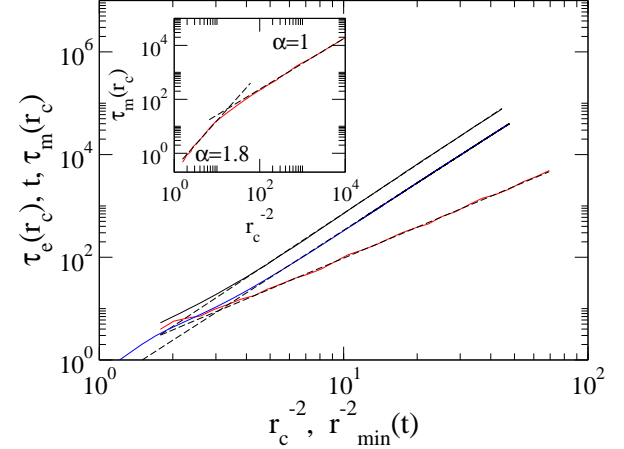


FIG. 3. For the two-vortex effective model of Eqs. (9,10,13), we plot $\tau_m(r_c)$ vs r_c^{-2} (top full line) and the time t vs $\langle r_{\min}^{-2}(t) \rangle$ (middle) along with power-law fits with respective exponent $\alpha \approx 3.1$ and $\alpha \approx 3.0$ (dashed lines). We also plot the escape time $\tau_e(r_c)$ (bottom) and a fit using $\alpha = 2$. These exponents are in good agreement with the predictions of Eqs. (17,21,23). For the three-vortex model (Insert), we plot $\tau_m(r_c)$ and power-law fits with exponent $\alpha \approx 1.8$ for “large” r_c (high density) and the predicted asymptotic exponent $\alpha = 1$, for $r_c \rightarrow 0$ (low density).

Reintroducing time and spatial units, we conclude that a purely two-body mechanism would lead to $\alpha = 3$ (see Eqs. (3,23)) and $\xi = 1/2$. Even if we assimilate the effective cut-off $r_0(t) \sim R(t/\tau)^{-1/4}$ to the vortex radius $a(t)$, we end up with $\alpha = 2$ and $\xi = 2/3$. We will show below that a three-body merging mechanism leads to a

faster density decay, and hence should dominate the dynamics at low vortex density. Actually, the inefficiency of the two-body merging processes has a simple physical interpretation suggested by our analytical results of Eqs. (14,15,17): when two like-sign vortices are at a distance $r \sim a \ll R$, they rotate around each other at such a high velocity ($d\varphi/dt \sim r^{-2}$) that the effective noise due to vortices at a distance greater than R (which has a correlation time of order $\tau \sim 1$, in our units) *is averaged out by the fast rotation*. In other words, the fast rotation makes the effective noise felt by both tagged vortices so weak that the two-body system becomes almost integrable (in the absence of noise, the distance between both vortices would remain strictly constant). This points to the necessity of the presence of at least another vortex at a distance of order a , in order to significantly perturb the nearly integrable two-body system.

By generalizing our model of Eqs. (9,10,13) to the case of 3 vortices (2 like-sign vortices and 1 of opposite sign), we define again $\tau_m(r_c)$ as the time for which the distance between both like-sign vortices reaches the value r_c for the first time. We numerically obtain that $\tau_m(r_c) \sim r_c^{-2}$ (see below for a theoretical argument), leading to $\alpha = 1$ and $\xi = 1$. The data are presented in the Insert of Fig. 3, confirming the results obtained in [20], although for a wider range of values of r_c . However, we find that the high density regime, corresponding to the largest values of r_c , is best fitted by $\alpha \approx 1.8$ (see Insert of Fig. 3). This value of α is associated to $\xi \approx 0.71$, in good agreement with (high density) simulations and experiments. Moreover, we find that when the two like-sign vortices are at a distance $r_c \ll 1$, the third (opposite-sign) vortex is at a distance proportional to r_c itself, justifying that this third vortex plays a crucial role in the collision process. Hence, we have shown that considering three-body merging processes speeds dramatically the dynamics, at least at sufficiently low densities $na^2 \ll 1$. This leads to a true scaling exponent $\xi = 1$ (associated with $\alpha = 1$). This regime is, however, difficult to reach in NS simulations and experiments, and we claim that only a pseudo-scaling is observed at the densities achieved, $na^2 \sim 0.1$. This corresponds to a transient regime with a pseudo-scaling exponent $\xi \simeq 0.71$ (associated with $\alpha \simeq 1.8$) measured on less than one decade. This pseudo-scaling exponent is expected to slowly increase with time, asymptotically reaching the true scaling exponent $\xi = 1$. A strong evidence that true scaling is not reached in the experiment of [23] is that the measured merging time was found to scale as $\tau_m \sim t^{0.57 \pm 0.12}$, instead of the necessary $\tau_m \sim t$. In addition, an indication that the exponent ξ measured in direct numerical simulations slowly increases with time is given in [17]. In order to reach the true scaling regime, one would need to run longer simulations with more vortices at the start which is difficult. Alternatively, a dynamical renormalization group analysis [20] allows one to reach very low densities more easily. In this case, it

is found that $\xi = 1$ (measured on four decades) in agreement with the present three-body kinetic theory.

Note that the local energy (see Eq. (5)) involving three vortices of respective circulation $\gamma, \gamma, -\gamma$, is $\mathcal{H}_3 \sim \gamma^2 \ln(r_{13}r_{23}/r_{12})$. It can remain finite and even constant even if $r_{12} \ll 1$, provided the third vortex of opposite sign is in the vicinity of the two merging vortices. In the case of a binary merging, the local energy $\mathcal{H}_2 \sim -\gamma^2 \ln(r_{12})$ diverges when $r_{12} \ll 1$ and the excess energy must be absorbed by the far away vortices, a very slow process, as shown in the present work. A similar argument explains why a three-vortex merging process involving three like-sign vortices is as inefficient as a two-body process, as observed numerically in [20]. Finally, we have confirmed numerically (simulation not shown) that adding a fourth vortex in our effective model does not change the scaling of the Insert of Fig. 3, provided that all four vortices do not have the same sign.

At low density $na^2 \ll 1$, the proposed physical picture is that ballistic dipoles collide with isolated vortices, the latter ultimately merging with the like-sign vortex of the dipole. We briefly recall the kinetic theory presented by two of us in [20] and generalize it to any dimension d , and in particular to geostrophic decaying turbulence of a three-dimensional stratified fluid [33], where planar vortices are replaced by almost spherical “blobs”. The vortex density satisfies an equation of the form $dn/dt = -n/\tau_m$ and, as already mentioned, the density power-law decay $n \sim t^{-\xi}$ implies $\tau_m \sim t$. Noting that the dipoles move almost ballistically with velocity $v_{dip} \sim \gamma/a \sim \omega a$ and using a classical cross section argument, we obtain

$$\tau_m \sim 1/(n_{dip} a^{d-1} v_{dip}), \quad (24)$$

where d is the dimension of space. Using a mean-field approximation, dipoles of typical size a are formed with a density $n_{dip} \sim n \times na^d$. Moreover, the energy $E \sim (\omega a)^2 na^d$ and the (potential) vorticity peak ω are conserved, so that Eq. (24) leads to

$$\tau_m \sim \omega^{-1} \left(\frac{\omega^2}{E} \right)^{\frac{2d}{d+2}} \times n^{-\frac{4}{d+2}}, \quad (25)$$

where we have kept track of the dimensional constants ω and E . Equivalently, this result can be rewritten in the same form as in Eq. (3)

$$\tau_m \sim \frac{\tau}{(na^2)^{\frac{6-d}{d+2}}} \quad (26)$$

Finally, expressing the asymptotic scaling condition, $\tau_m \sim t$, Eqs. (25,26) lead to

$$\xi = \frac{d+2}{4}, \quad \alpha = \frac{6-d}{d+2}. \quad (27)$$

In $d = 2$, we obtain $\xi = 1$ (associated to $\alpha = 1$), which agrees with the numerical results of Fig. 3. Again, this

value is slightly higher than the exponents measured in experiments and most numerical simulations. However, we have already argued that the smallest area fraction na^2 reached remains quite large, except in the RG procedure of [20], which indeed found $\xi \approx 1$. In the experiment of [23], the measured merging time was found to scale as $\tau_m \sim t^{0.57 \pm 0.12}$, instead of the necessary $\tau_m \sim t$, showing that the scaling regime was not yet attained. However, we observe that the theoretical relation of Eq. (25) is remarkably well verified in this experiment:

$$\tau_m \sim t^{0.57 \pm 0.12} \sim \frac{\omega}{E} \times n^{-1} \sim t^{0.55 \pm 0.14}. \quad (28)$$

This suggests that the result of Eq. (25) could be valid in a wider range of time, even before reaching the true asymptotic scaling regime. This phenomenon is actually quite common in the context of critical phenomena, when dealing with finite-size samples and simulation time: the scaling relations between critical physical quantities (like the susceptibility or the correlation length/time in magnetic systems) are often found to be better obeyed numerically than between these quantities and the critical parameter itself (*e.g.* the distance to the critical temperature $|T - T_c|$).

In $d = 3$, we obtain $\xi = 5/4$ (associated to $\alpha = 3/5$), in good agreement with the value $\xi \simeq 1.25 \pm 0.10$ measured in NS simulations of geostrophic decaying turbulence in a stratified fluid [33]. We argue that due to the fastest decay in $d = 3$, the low density regime where the three-body mechanism sets in appears faster. In addition, the increased dimensionality generally plays in favor of a better validity of a mean-field treatment.

In conclusion, we have presented an effective theory for the merging of two vortices advected by the effective noise of the other vortices. Several quantities including the merging time τ_m and the *pdf* $P(r, t)$ have been derived analytically and are in excellent agreement with numerical simulations. The results of this study point to the weak efficiency of two-body processes, as the fast rotation of the vortex pair averages out the effective advecting noise due to the other vortices. We numerically find that a similar effective theory, where three vortices of different sign now participate to the merging process, leads to a faster decay of the density, $n(t) \sim t^{-1}$, after a transient regime where $n(t) \sim t^{-0.71}$. We therefore conclude that three-body processes should dominate, at least at small vortex density. This result can be understood within a simple mean-field kinetic theory describing the merging process as the collision of a ballistic dipole with an isolated vortex. This same theory applied to geostrophic turbulence in three dimensions leads to $n(t) \sim t^{-5/4}$, in good agreement with numerical simulations. It would be certainly interesting to generalize this study for an increasing number $N > 4$ of tagged vortices, yet small enough for the numerical simulations to reach very small effective densities (*i.e.* small r_c). The N vortex mutual

dynamics would still be treated exactly, but in the effective noisy background generated by all the other vortices.

Appendix A: Conservation of the vorticity peak

It is numerically observed that the vorticity peak is almost conserved in 2D decaying turbulence [12], an important ingredient of the scaling theory. In this Appendix, we would like to motivate this claim in terms of statistical mechanics and kinetic theory of the 2D Euler equation.

The Miller-Robert-Sommeria (MRS) statistical theory [36, 37] is relatively well-suited to describe the rapid merging of two vortices. Knowing the initial condition and assuming ergodicity (efficient mixing) the statistical theory predicts the shape of the new vortex resulting from this merging. Furthermore, the mixing process can be described in terms of relaxation equations [38] obtained from a maximum entropy production principle (MEPP). Assuming, for simplicity, that the initial vortices have a uniform vorticity $\omega = \sigma_0$, the relaxation equations can be written

$$\frac{\partial \bar{\omega}}{\partial t} + \mathbf{u} \cdot \nabla \bar{\omega} = \nabla \cdot [D(\mathbf{r}, t) (\nabla \bar{\omega} + \beta(t) \bar{\omega}(\sigma_0 - \bar{\omega}) \nabla \psi)], \quad (29)$$

$$\beta(t) = -\frac{\int D(\mathbf{r}, t) \nabla \bar{\omega} \cdot \nabla \psi \, d\mathbf{r}}{\int D(\mathbf{r}, t) \bar{\omega}(\sigma_0 - \bar{\omega}) (\nabla \psi)^2 \, d\mathbf{r}}, \quad (30)$$

where $\bar{\omega}(\mathbf{r}, t)$ is the coarse-grained vorticity field and $D(\mathbf{r}, t)$ the “turbulent” diffusion coefficient. If $D(\mathbf{r}, t)$ is constant, the relaxation equations converge towards the statistical equilibrium state given by a Fermi-Dirac-like distribution

$$\bar{\omega}(\mathbf{r}) = \frac{\sigma_0}{1 + e^{\sigma_0(\beta \psi(\mathbf{r}) + \alpha)}}. \quad (31)$$

However, it has been observed at several occasions (see, *e.g.*, [39, 40]) that relaxation is *incomplete* due to lack of ergodicity. This is clearly a limitation of the statistical theory. In order to take incomplete relaxation into account, it has been proposed that the diffusion coefficient $D(\mathbf{r}, t)$ varies in space and time. Qualitative arguments [41], or more sophisticated kinetic theory [42], indicate that the diffusion coefficient should be proportional to the local variance $\omega_2 = \bar{\omega}^2 - \bar{\omega}^2 = \bar{\omega}(\sigma_0 - \bar{\omega})$ of the vorticity fluctuations. It must also decrease in time as the fluctuations decay. Therefore

$$D(\mathbf{r}, t) = A(t) \bar{\omega}(\mathbf{r}, t) [\sigma_0 - \bar{\omega}(\mathbf{r}, t)], \quad (32)$$

where $A(t)$ tends to zero on a few dynamical times. In the “mixing zone” where the fluctuations are strong, the diffusion coefficient is large and the system rapidly reaches a Fermi-Dirac-like distribution (31), with an inverse temperature β' and a chemical potential α' that may be different from the equilibrium ones. On the other hand,

from Eq. (32), one sees that the diffusion coefficient is small in the regions where the fluctuations are weak. This concerns the core of the vortex ($\bar{\omega}(\mathbf{r}, t) \rightarrow \sigma_0$) where the vorticity is maximum and the region surrounding the vortex ($\bar{\omega}(\mathbf{r}, t) \rightarrow 0$) which is not sampled by vorticity. Therefore, the relaxation towards the Fermi-Dirac-like distribution (31) will be very slow in these regions. Since, in parallel, the diffusion coefficient decreases with time (because of the term $A(t)$), the system will not have time to reach the Fermi-Dirac-like distribution in these regions. Therefore, mixing will be relatively inefficient in the core and at the periphery of the vortex. These arguments of kinetic theory may explain why the vorticity peak is relatively well conserved during a merging and why the vortex is more confined than what the statistical theory predicts assuming *complete* mixing. These arguments have been developed in Sec. 4.3 of [43].

Appendix B: The Fokker-Planck equation

In order to write down the Fokker-Planck equation associated with the stochastic process defined by Eqs. (9,10,13), it may be simpler to use cartesian coordinates. Equations (9,10) are therefore rewritten as

$$\frac{dx}{dt} = -\frac{y}{r^2} + x\eta_\alpha + y\eta_\beta, \quad (33)$$

$$\frac{dy}{dt} = \frac{x}{r^2} - y\eta_\alpha + x\eta_\beta. \quad (34)$$

Introducing the convenient notations $\mathbf{r} = (x, y)$ and $\mathbf{w} = (\eta_\alpha, \eta_\beta)$, the Fokker-Planck equation for $P(\mathbf{r}, \mathbf{w}, t)$ is

$$\begin{aligned} \frac{\partial P}{\partial t} + \frac{\partial}{\partial x} \left[\left(-\frac{y}{r^2} + x\eta_\alpha + y\eta_\beta \right) P \right] + \\ \frac{\partial}{\partial y} \left[\left(\frac{x}{r^2} - y\eta_\alpha + x\eta_\beta \right) P \right] = \frac{\partial}{\partial \mathbf{w}} \cdot \left(\frac{\partial P}{\partial \mathbf{w}} + P \mathbf{w} \right). \end{aligned} \quad (35)$$

The stationary solution ($\partial_t P = 0$) of this Fokker-Planck equation is obtained when the r.h.s. and the l.h.s. vanish individually. The cancelation of the r.h.s. implies that

$$P_s(\mathbf{r}, \mathbf{w}) = C(\mathbf{r}) e^{-w^2/2}. \quad (36)$$

Inserting this expression in the l.h.s. of the Fokker-Planck equation, we obtain $C(\mathbf{r}) = \text{constant}$. Therefore,

$$P_s(\mathbf{r}, \mathbf{w}) \propto e^{-w^2/2}. \quad (37)$$

It is noteworthy that the steady state of this Fokker-Planck equation is spatially homogeneous, *i.e.* $P_s(\mathbf{r}) = \text{constant}$, and $P_s(r) = r$ in radial coordinates.

- [1] P. Tabeling, Phys. Rep. **362**, 1 (2002).
- [2] B. Fornberg, J. Comput. Phys. **25**, 1 (1977).
- [3] C. Basdevant, B. Legras, R. Sadourny, and M. Béland, J. Atmos. Sci. **38**, 2305 (1981).
- [4] J. C. McWilliams, J. Fluid Mech. **146**, 21 (1984).
- [5] R. Benzi, S. Patarnello, and P. Santangelo, J. Phys. A **21**, 1221 (1988).
- [6] J. C. McWilliams, J. Fluid Mech. **219**, 361 (1990).
- [7] G. L. Brown and A. Roshko, J. Fluid Mech. **64**, 775 (1974).
- [8] H. Aref and E. D. Siggia, J. Fluid Mech. **100**, 705 (1980).
- [9] Y. Couder, C. R. Acad. Sc. Paris **297**, 641 (1983).
- [10] B. Legras, P. Santangelo, and R. Benzi, Europhys. Lett. **5**, 37 (1988).
- [11] M. V. Melander, N. J. Zabusky, and J. C. McWilliams, J. Fluid Mech. **195**, 303 (1988).
- [12] G. F. Carnevale, J. C. McWilliams, Y. Pomeau, J. B. Weiss, and W. R. Young, Phys. Rev. Lett. **66**, 2735 (1991).
- [13] J. B. Weiss and J. C. McWilliams, Phys. Fluids A **5**, 608 (1993).
- [14] A. Bracco, J. C. McWilliams, G. Murante, A. Provenzale, and J. B. Weiss, Phys. Fluids **12**, 2931 (2000).
- [15] H. J. H. Clercx and A. H. Nielsen, Phys. Rev. Lett. **85**, 752 (2000).
- [16] L. J. A. van Bokhoven, R. R. Trieling, H. J. H. Clercx, and G. J. F. van Heijst, Phys. Fluids **19**, 046601 (2007).
- [17] J.-P. Laval, P.-H. Chavanis, B. Dubrulle, and C. Sire, Phys. Rev. E **63**, 065301 (2001).
- [18] D. G. Dritschel, R. K. Scott, C. Macaskill, G. A. Gottwald, and C.V. Tran, Phys. Rev. Lett. **101**, 094501 (2008).
- [19] R. Benzi, M. Colella, M. Briscoloni, and P. Santangelo, Phys. Fluids A **4**, 1036 (1992).
- [20] C. Sire and P.-H. Chavanis, Phys. Rev. E **61**, 6644 (2000).
- [21] P. Tabeling, S. Burkhart, O. Cardoso, and H. Willaime, Phys. Rev. Lett. **67**, 3772 (1991).
- [22] O. Cardoso, D. Marteau, and P. Tabeling, Phys. Rev. E **49**, 454 (1994).
- [23] A. E. Hansen, D. Marteau, and P. Tabeling, Phys. Rev. E **58**, 7261 (1998).
- [24] H. J. H. Clercx, G. J. F. van Heijst, and M. L. Zoeteweij, Phys. Rev. E **67**, 066303 (2003).
- [25] G. K. Batchelor, Phys. Fluids Suppl. II **12**, 233 (1969).
- [26] Y. Pomeau, J. Plasma Phys. **56**, 3 (1996).
- [27] C. Sire, J. Tech. Phys. **37**, 563 (1996).
- [28] T. Iwayama, H. Fujisaka, and H. Okamoto, Prog. Theor. Phys. **98**, 1219 (1997).
- [29] E. Trizac, Europhys. Lett. **43**, 671 (1998).
- [30] V. Yakhot and J. Wanderer, Phys. Rev. Lett. **93**, 154502 (2004).
- [31] J. H. LaCasce, Phys. Fluids **20**, 085102 (2008).
- [32] G. Kirchhoff, *Lectures in Mathematical Physics, Mechanics* (Teubner, Leipzig, 1877).
- [33] J. C. McWilliams, J. B. Weiss, and I. Yavneh, J. Fluids Mech. **401**, 1 (1999).
- [34] D. G. Dritschel and N. J. Zabusky, Phys. Fluids **8**, 1252 (1996).
- [35] J. B. Weiss, A. Provenzale, and J. C. McWilliams, Phys. Fluids **10**, 1929 (1998).
- [36] J. Miller, Phys. Rev. Lett. **65**, 2137 (1990).
- [37] R. Robert and J. Sommeria, J. Fluid Mech. **229**, 291 (1991).

* clement.sire@irsamc.ups-tlse.fr ; chavanis@irsamc.ups-tlse.fr

- [38] R. Robert and J. Sommeria, Phys. Rev. Lett. **69**, 2776 (1992).
- [39] P. Chen and M. C. Cross, Phys. Rev. Lett. **77**, 4174 (1996).
- [40] H. Brands, P.-H. Chavanis, R. Pasmanter, and J. Sommeria, Phys. Fluids **11**, 3465 (1999).
- [41] R. Robert and C. Rosier, J. Stat. Phys. **86**, 481 (1997).
- [42] P.-H. Chavanis, Phys. Rev. Lett. **84**, 5512 (2000).
- [43] P.-H. Chavanis, Physica A **387**, 1123 (2008).